THE ELECTROSPRAY: FUNDAMENTALS AND COMBUSTION APPLICATIONS

Alessandro Gomez
Department of Mechanical Engineering
Yale University
New Haven, Connecticut 06520

1. Introduction

Liquid fuel dispersion in practical systems is typically achieved by spraying the fuel into a polydisperse distribution of droplets evaporating and burning in a turbulent gaseous environment. In view of the nearly unsurmountable difficulties of this two-phase flow, it would be useful to use an experimental arrangement that allow a systematic study of spray evolution and burning in configurations of gradually increasing levels of complexity, starting from laminar sprays to fully turbulent ones. An Electrostatic Spray (ES) of charged droplets lends itself to this type of combustion experiments under well-defined conditions and can be used to synthesize gradually more complex spray environments. In its simplest configuration, a liquid is fed into a small metal tube maintained at several kilovolts relative to a ground electrode few centimeters away. Under the action of the electric field, the liquid meniscus at the outlet of the capillary takes a conical shape, with a thin jet emerging from the cone tip. This jet breaks up farther downstream into a fine spray of charged droplets (see Fig. 1 and ref. 1). Several advantages distinguish the electrospray from alternative atomization techniques: the self-dispersion property of the spray due to coulombic repulsion; the absence of droplet coalescence; the potential control of the trajectories of charged droplets by suitable disposition of electrostatic fields; and the decoupling of atomization, which is strictly electrostatic, from gas flow processes. Furthermore, as recently shown in our laboratory (ref. 2), the electrospray can produce quasi-monodisperse droplets over a very broad size range (1-100 μm).

The ultimate objective of this research project is to study the formation and burning of electrosprays of liquid fuels first in laminar regimes and then in turbulent ones. Combustion will eventually be investigated in conditions of three-dimensional droplet-droplet interaction, for which experimental studies have been limited to either qualitative observations in sprays or more quantitative observations on simplified systems consisting of a small number of droplets or droplet arrays (refs. 3-6). The compactness and potential controllability of this spray generation system makes it appealing for studies to be undertaken in the next two years on electrospray combustion in reduced-gravity environments such as those achievable at NASA microgravity test facilities.

2. Summary of the Research Activity from 3-1-1991 to 8-31-1992

The project has developed along two parallel avenues: we have performed a variety of cold flow experiments aimed at examining the fundamental mechanism of electrospray atomization and dispersion as well as identifying and characterizing the domain of operating variables under which the generated droplets are quasi-monodisperse. The other focus of the research has been on the combustion of the electrospray in laminar regime: we have constructed a counterflow spray burner, tested it at normal gravity and begun to examine the dynamics of the interaction of droplets and flame. Primary diagnostic tools are: a commercial Phase Doppler Anemometer (PDA), the workhorse of this phase of the project, used to measure distributions of droplet size and either axial or radial velocity component; and a shadowgraph system consisting of a nanosecond flashlamp, a long-range microscope and a CCD camera, capable of capturing and digitizing images of droplet shadows with an overall magnification of up to 1100X. Further details are given in the seven publications (refs. 2, 7-12) that have resulted from the research activity in the first seventeen months of the project.

2.1 Fundamentals of Electrospray Atomization

Research on the fundamentals of electrospray atomization is crucial to develop strategies for optimizing the ES and tailoring it to a particular application. In particular, it is necessary to: define and understand limits of operation of the system; infer scaling laws that would allow to generalize experimental findings and perform scale-up to commercially interesting liquid flow-rates. In this phase of the study we first obtained a phenomenological picture of the atomization and dispersion processes, as sketched in Fig. 1, through flash shadowgraphs of the breakup region (refs. 2 and 10). When narrow size distributions are generated, the liquid exits the cone formed at the outlet of the charged capillary as a thin, stable, thread that persists for a short distance. This ligament then breaks up into droplets of bimodal size distribution, with primary, larger droplets, and satellite ones, on average one third smaller. Farther downstream, droplets in the spray core become nearly monodisperse as the satellites, driven by the electric field, migrate more rapidly away from the spray axis because of higher charge to mass ratio and lower inertia. The core of uniform droplets was found to carry 97% of the total flow rate and 85% of the total current; the remainder is present in a shroud of satellites. We also identified the operating conditions under which the electrospray generates monodisperse droplets. A map of the ES stability domain in the applied-voltage vs liquid flow rate plane was obtained for heptane, doped with the antistatic additive (Stadis 450,

0.3% by weight) to provide electric conductivity. A domain was identified in which monodisperse droplets were generated whose size was primarily controlled by the liquid flow rate and, to a less extent, by the applied voltage (ref. 12). Since the ultimate goal was to evaluate the size and monodispersity of the spray, results are plotted in Fig. 2 as average droplet diameter, measured by the PDA versus applied voltage for several liquid flow rates. For all measurements the droplet standard deviation was less than 10 % of the average diameter, the latter spanning a remarkable range of over two orders of magnitude (1-140 μm). The boundaries of this stability region were found to be determined by the onset of different types of instabilities: at a given flow rate, the minimum voltage was set by the onset of pulsations in the liquid meniscus, whereas the maximum voltage was typically set by the onset of traverse instabilities on the jet issuing from the conical meniscus. The lower flow rate limit was set by diagnostic limitations: the Phase Doppler system cannot, in fact, measure submicron droplets; the upper limit in flow rate was instead determined by the onset of droplet fission, which is achieved when Coulomb repulsion of the electrical charges on the droplet surface overcomes surface tension and the droplet disrupts, as discussed below in greater detail.

We also examined in detail a prototypical ES, operated for diagnostic convenience in conditions resulting in the generation of monodisperse droplets measuring 32 μm in diameter. After detailed scans of the spray in both radial and axial directions, we first observed that droplet velocity and number density profiles are self-similar in the electrospray. Efforts were then focused on the inference of the electric field that is the driving force determining spray formation and dispersion. Such determination is important for spray modelling, it can help the analysis of the complex electro-hydrodynamics in the liquid meniscus and it is also useful to define limits of operation of the system. The electric field was determined indirectly by quantifying through a variety of measurements on the charged droplets the electrostatic force acting on them (ref. 10). To this end, we: a) measured both droplet and gas velocity, droplet size and average interdroplet spacing; b) inferred droplet charge from measurements of the total current carried by monodisperse droplets using a specially fabricated, variable-aperture electrode; and c) solved the equation of motion for an isolated droplet under the action of electrostatic, gravitational and drag forces. We found that droplets, driven by the field, are ejected from the jet at relatively high velocity. They maintain this velocity even though the field is rapidly decreasing because of inertia effects and ultimately decelerate under the action of drag force and a progressively weaker electrostatic force. The net electric field acting on the droplet is due primarily to the external field, except near the break-up region of the spray, where the internal field due to space charge appears also to be important. Indeed, droplet coulombic repulsion plays a crucial role: if only the external field were acting on the droplets, they would predominantly persist in their axial trajectory without dispersing into a spray. Space charge effects, coupled with diverging lines of the external field between capillary and ground electrode ultimately lead to spray dispersion.

2.2 Electrospray Combustion

Spray combustion in a stagnation-point flow configuration has been examined experimentally, numerically and analytically in diffusion flames in a few recent studies (refs. 13-17). The focus of our effort has been to study the effects of the interaction between flow field, flame and droplets on the structure of the counterflow spray diffusion flame (ref. 7). We also found the first evidence in a burning spray of secondary atomization due to Coulomb fission (ref. 11).

The counterflow diffusion flame burner (Fig. 3) has been described elsewhere (ref. 7). Briefly, electrosprayed heptane and a co-flow of N_2 flowed through the bottom half of the burner and oxygen was admitted through the top one. Combustion occurred in a gap between top and lower half of the burner, near the stagnation region between the two impinging streams. Experiments were performed on two heptane flames, both operated at the same overall equivalence ratio of 0.36, and, thus, both having the same adiabatic flame temperature. The first flame, labelled LS, was characterized by a nominal strain rate of 3 s^{-1}, droplet mean diameter and mean velocity near the burner mouth equal to 36.3 μm and 0.63 m/s respectively. In the second flame, labelled HS, strain rate, initial droplet size and droplet relative velocity were increased to 4.3 s-1, 47.3 μm and 1.3 m/s respectively. The ratio of standard deviation and mean droplet size near the burner mouth were 0.09 and 0.13 in the two flames and therefore droplets can be considered quasi-monodisperse, at least initially. Both flames are in a diluted spray regime where droplet-droplet interactions are expected to be negligible (ref. 18). Droplets entered the combustion region with a substantial slip with respect to a host gas velocity of only a few cm/s.

In Fig. 4 the average droplet diameter and gas-phase temperature, measured along the burner axis, are plotted versus the distance from the bottom burner rim, z, for the two heptane flames: open symbols refer to Flame LS (Low Strain rate) and full symbols to Flame HS (High Strain rate). The error bars on the droplet diameter have a width equal to two standard deviations. The temperature was measured with a fine silica coated, Pt-Pt/13%Rh thermocouple. In the case of Flame LS, we observe that as droplets approach the combustion region and the stagnation plane, the temperature begins to rise and droplet mean diameter decreases gently in the first 4.5 millimeters and much more abruptly in the subsequent two millimeters. Droplets disappear at about 5.7 mm from the burner mouth, before reaching the flame that was located at z=7 mm and appeared like a thin, flat sheet, of a blue-violet color. In the case of the higher strain rate heptane flame, HS, the flame had an appearance markedly different from Flame LS and exhibited a more complex structure. We observe a thin blue region, similar to that of Flame LS, at z=7.1 mm, another thin sheet characterized by violet luminescence at z=7.3 mm and a thick orange region between z=7.7 and z=9.6 mm, whose luminosity is presumably due to the presence of soot particles. Some of the droplets penetrated through the blue flame and continued to burn within the oxidizer region where they eventually disappeared in the homogeneously thick orange region. Larger droplets burning individually could be identified by their luminous wake occasionally protruding beyond the uniform orange region. From these measurements one concludes that Flame LS behaves in some respects as a purely gaseous diffusion flame

since droplets never directly interact with the flame but simply provide a source of heptane vapor, which then diffuses towards the oxidizer region. This observation confirms numerical predictions under similar conditions (refs. 14, 17) and is also consistent with visual observations of analogous spray flames (ref. 15, 17). Flame HS on the other hand clearly exhibit a direct interaction of droplets and flame. The dramatically different appearance of the two flames can be explained as follows. First, in the case of Flame HS the droplet mean size and axial velocity component measured close to the burner mouth are 30 % larger and twice as large as compared to Flame LS. The larger size and larger velocity of droplets in HS result in longer lifetime (based on d-square law) and shorter residence time, which accounts for droplet survival over significantly longer distances as compared to Flame LS. Second, inertia effects and the consequent inability of the droplets to follow the host gas are more significant in the higher strain rate flame.

A comparison between the temperature profiles in the two heptane flames (Fig. 4) shows that the flame with the nominally higher strain rate, Flame HS has a substantially broader temperature profile. This finding is in contrast with what expected in purely gaseous diffusion flames on the basis of both theoretical analyses, that predict proportionality between the width of the temperature profile and the inverse of the square root of the strain rate (ref. 19), and numerical predictions (ref. 20). Furthermore, even though the two flames have identical overall equivalence ratios and nearly equal adiabatic flame temperatures, Flame HS has a peak temperature 240 K higher than Flame LS. This difference is probably an effect of the local stoichiometry. Since N_2 was introduced only from the fuel side, the inert concentration is a monotonically decreasing function of z. Thus, droplets cross the blue flame in Flame HS and continue to burn stoichiometrically in an oxygen rich environment while the inert concentration progressively decreases.

The error bars on the droplet diameters in Fig. 3 show that the initially narrow size distribution broadens in the course of evaporation. This effect can be attributed to size-dependent droplet evaporation rate and residence time, as explained in detail in ref. 7. Also noteworthy is the non-monotonic behavior in Flame HS of the mean droplet diameter as function of the axial coordinate, z, which is due to an inertia separation effect (ref. 7).

2.3 Fission of charged Droplet

Measurements of charge and size of droplets generated in electrostatic sprays of heptane operated in the conditions described in Section 2.1 showed that: a) droplet charge-to-volume ratio is a monotonically decreasing function of droplet size; and b) that the larger are the droplets the closer they are to the limiting charge at which they rupture. This limit is attained when the Coulombic repulsion of surface charge overcomes surface tension (ref. 21). Thus, somewhat paradoxically, large droplets with relatively low charge-to-volume ratio are proner to disintegrate than smaller droplets with higher ratios. Exploiting these findings, for the first time we have captured photographically the fission of nearly-monodisperse, charged droplets generated by an electrospray (Fig. 5). Observed fissile patterns show that droplet disintegration is characterized by the formation of a tail, or "cone", reminiscent of the conical liquid meniscus from which the electrospray originates (see Fig. 1). From the tip of this cone, a stream of droplets is ejected, all much smaller in size than the parent droplet and apparently equisized. Consequently, since droplet evaporation time varies with the square of the droplet diameter at typical prevailing conditions, the offspring droplets will vaporize at much faster rate than will the residual "parent" droplet. A phenomenological explanation of the observed dependence of charge density on droplet size has been offered in terms of the relative magnitude of two characteristic times: an electric relaxation time, i.e. a characteristic time for charge motion in the liquid or on the liquid surface; and a characteristic fluid time, i.e. the time over which varicose wave instabilities propagate along the axis of the liquid jet from which the electrospray originates. Some implications of these findings, with particular emphasis to electrospray ionization, a technique widely used in biochemical mass-spectrometry are discussed in (ref. 9).

Experimental evidence of droplet fission was also obtained in the combustion of electrosprays (ref. 11). PDA measurements in the flame labelled LS in Fig. 4 showed in fact a peculiar feature of the size distributions in the vicinity of the flame. Fig. 6 shows one such distribution as measured at z= 5.5 mm. Notice the bimodality of the distribution with the appearance of a secondary peak in correspondence of diameters of 2-3 μm, i.e. one order of magnitude smaller than the mean droplet diameter. No evaporation mechanism can account for this finding, which can be explained only in terms of a disintegration of droplets into finer fragments of consistently much smaller size. Other evidence in support of the existence of secondary atomization is offered by velocity measurements showing that in correspondence with secondary peaks in the size distribution both radial and axial components of the droplet velocity are unusually large, i.e. one or two orders of magnitude larger than the corresponding mean values, which is indicative of the occurrence of an ejection process. This disruption occurs despite the presence of chemi-ions and electrons that are naturally present in the flame and that might have partially or totally neutralized the droplet, as originally suggested by Weinberg (ref. 22). The morphology of the fission process captured in cold flow experiments (Fig. 5) is consistent with the size distribution found in these combustion experiments.

3.0 Future Plans

Task 1- We would like first to characterize as quantitatively as possible the evolution of the spray as the droplets approach the flame. With the measurements of droplet size, velocity and gas-phase temperature, we should to be able to reconstruct the evolution of the droplet size distribution as the droplets approach the flame and to determine the droplet vaporization rate.

Task -2 Further studies are needed to capture droplet fission in combustion environments and to clarify whether disruption is characterized by only 1-2 % liquid mass loss, or whether the mass loss can be substantially higher because of the presence of chemi-ions*. In the first case, the disruption process enhances the evaporation rate of only a small fraction of the liquid supply but it may still aid in the overall stability of the spray flame. In the second case, the advantages of secondary atomization would be far more dramatic. A suitable electrostatic atomizer would generate *directly* large droplets, with the inherent advantage of good penetration of fuel into the oxidizer, and *indirectly* small droplets, via Coulombic fission,with the advantage of rapid evaporation and effective molecular mixing of fuel and oxidizer.

Task 3- Experiments to date have been conducted in a regime of diluted spray, as discussed in Section 2.2. To operate the spray ultimately in a regime of droplet-droplet interaction, we would like to develop strategies to focus electrostatically the spray by manipulating droplet trajectories with electric fields and therefore controlling interdroplet spacing If space charge effects are limiting, partial neutralization of droplet charge by an aerosol neutralizer may be necessary before focusing can be implemented.

Task 4 - Part of the experimental program in the third and fourth year would be implemented at the 2s Drop Tower NASA facility. Efforts will be made to retrofit the current version of the counterflow burner to the drop-package before the end of the current year. The obvious goal is that of studying spray combustion in an environment free of natural convection effects. Buoyancy can generally play a role in displacing the flame in low strain rates flames, as we also observed in purely gaseous flames (ref. 24). In the particular case of spray flames, its role will become very significant in regimes of droplet-droplet interaction, when the characteristic length of the Grashof number is no longer the droplet size but the "spray size." In this context, efforts in task 3 will be crucial.

Task 5- To be able to compare the results of the laminar spray experiments in the counterflow configuration with computations, Prof. M. D. Smooke will develop a model that accounts for the interchange of mass, momentum, chemical species and energy between the gas and liquid phases in a monodisperse spray. Building upon the experience obtained in the investigation of detailed transport/finite rate chemistry models of gaseous premixed and nonpremixed counterflow systems (refs. 20, 25, 26), we plan to solve the complete liquid-gas phase system with a modified version of the algorithm described in detail in the literature (ref. 25), after coupling in the liquid phase by utilizing the ideas of Sirignano and coworkers (ref. 14). This approach will enable us to investigate the effects of droplet size, droplet spacing and the effects of droplet vaporization on flame location, temperature and species distributions. The interaction between modeling and experiments will help in interpreting the experimental findings and in validating the model both at normal and reduced gravity.

Task 6- We plan to complement the measurements of droplet size and velocity with spectroscopic determination at normal gravity of the concentration of major gaseous species as well as of some radicals. This study will be valuable for determining flame location, studying its evolution, evaluating oxidizer penetration into the droplet-laden region and comparing results with numerical predictions. Experiments will be performed in collaboration with Prof. M. B. Long. Major species such as O_2, CO_2, H_2O and N_2 will be detected by spontaneous Raman scattering. For radical such as OH and CH, on the other hand, the laser will be tuned to an absorption line and the fluorescence will be detected at a wavelength shifted from that of the input laser. Point measurements can be performed by using optical filters to reject partially or totally the droplet intense elastic light scattering in combination with a synchronization scheme in which spectroscopic signals will be collected conditionally upon the absence of droplets in the laser probe volume. Since the anticipated interdroplet spacings are in the order of ten droplet diameters and droplet data rate are in the order of a few Hz, this strategy should be easily realizable. We would also like to initiate imaging experiments by combining a CCD detector with a pulsed laser illumination sheet or line and ultimately map the concentrations in a single plane or line intersecting the spray (see for example ref. 27).

Task 7- The last phase of the project will be devoted to turbulent sprays. The same type of measurements performed in laminar sprays will be repeated in carefully selected environments in which turbulence is "injected" in the gaseous stream by synthesizing various turbulent scenarios, characterized by different intensities and scales. Since liquid atomization is achieved strictly by charging, in contrast with aerodynamic atomization mechanisms, the host gas where the liquid is injected can in fact be controlled independently.

4.0 References

1. Zeleny, *J., Phys. Rev.* **10**, p.1 (1917).
2. Gomez, A. and Tang, K., Proceedings of the Fifth International Conference on Liquid Atomization and Spray Systems, ICLASS-91, Gaithersburg, MD, U.S.A., H. G. Semerjian Ed., NIST Special Publication No. 813, p.805 (1991).
3. Twardus, E.M. and Brzustowki, T.A., *Combust. Sci. and Technol.*, **17**, p.215 (1978).
4. Brzustowski, T.A., Twardus, E.M., Wojcicki, S. and Sobiesiak, A., *AIAA J.*, **17**, p.1234 (1979).
5. Sangiovanni, J.J. and Kesten, A.S., *Sixteenth Symposium (International) on Combustion*, p.577, The Combustion Institute (1977).
6. Sangiovanni, J.J. and Labowski, M., *Combust. Flame*, **47**, p.15 (1982).

* Taflin et al. (ref. 23), in fact, reported that in ionized gaseous medium the disruption can differ substantially from that in unionized gases and can be characterized by much larger mass loss.

7. Chen, G. and Gomez, A., "Counterfow Diffusion Flames of Quasi-Monodisperse Electrostatic Sprays," to appear in *Twenty-fourth Symposium (International) on Combustion*, (The Combustion Institute, Pittsburgh, PA, 1992).
8. Gomez, A. and Tang, K., Proceedings of the Fifth International Conference on Liquid Atomization and Spray Systems, ICLASS-91, H. G. Semerjians, Eds., (NIST Special Publication 813, Gaithersburg, MD,USA, p.805, 1991).
9. Gomez, A. and Tang, K., "Fission of Charged Droplets in Electrostatic Sprays", submitted to *Phys. Fluids A* (1992).
10. Tang, K. and Gomez, A.: "On the Structure of an Electrostatic Spray of Monodisperse Droplets", submitted to *Phys. Fluids A* (1992).
11. Gomez, A. and Chen, G., "Secondary Atomization in the Combustion of Electrostatic Sprays," submitted to *Combust. and Flame* (1992).
12. Gomez, A. and Tang, K., "Stability Domain of an Electrospray Generating Monodisperse Droplets in the Size Range 1-140 μm", to appear in *J. Aerosol Sci.* (1992).
13. Greenberg, J.B., Albagli, D. and Tambour, Y., *Combust. Sci. and Tech.*, **50**, p. 255 (1986).
14. Continillo, G. and Sirignano, W.A., *Comb. Flame* **81**, p.325 (1990).
15. Li, S.C., Libby, P.A. and Williams, F.A. "Experimental and Theoretical studies of Counterfow Spray Diffusion Flames," to appear in *Twenty-fourth Symposium (International) on Combustion*, (The Combustion Institute, Pittsburgh, PA, 1992).
16. Chen, N. H., Rogg, B. and Bray, K.N.C., "Modelling Laminar Two-phase Counterflow Flames with Detailed Chemistry and Transport", to appear in *Twenty-fourth Symposium (International) on Combustion*, (The Combustion Institute, Pittsburgh, PA, 1992).
17. Lacas, F., Darabiha, N., Verasevel, P., Rolon, J.C. and Candel, S., "Influence of Number Density on the Structure of Strained Laminar Spray Flames", to appear in *Twenty-fourth Symposium (International) on Combustion*, (The Combustion Institute, Pittsburgh, PA, 1992).
18. Faeth, G.M., *Prog. Energy Combust. Sci.* **9**, p.1 (1983).
19. Zeldovich, Ya.B., Barenblatt, G.I., Librovich, V.B. and Makhviladze, G.M.: The Mathematical Theory of Combustion and Explosions, Ch. 8, Plenum (1985).
20. Puri, I.K., Seshadri, K., Smooke, M.D. and Keyes, D.E., *Combust. Sci. and Tech.* **56**, p.1 (1987).
21. Rayleigh, *Philos. Mag.* **14**, p.184 (1882).
22. Thong, K.C. and Weinberg, F.J., *Proc. Roy. Soc. Lond. A* **324**, p.201 (1971).
23. D. C. Taflin, T. L. Ward and E. J. Davis, *Langmuir* **5**, p.376 (1989).
24. Gomez, A. and Rosner, D. E., "Thermophoretic Effects on Particles in Counterflow Laminar Diffusion Flames," to appear in *Combust. Sci. and Tech.* (1992).
26. Giovangigli, V. and Smooke, M. D., *Comb. Sci. and Tech.*, **53**, p.23 (1987).
25. Smooke, M. D., Puri, I. K. and Seshadri, K., *Twenty-First Symposium (International) on Combustion*, p. 1783, The Combustion Institute, 1987.
26. Giovangigli, V. and Smooke, M. D., *Comb. Sci. and Tech.*, **53**, p.23 (1987).
27. Smooke, M. D., Lin, P., Lam, J. K. and long, M.B., *Twenty-Third Symposium (International) on Combustion*, p. 575, The Combustion Institute, 1991.

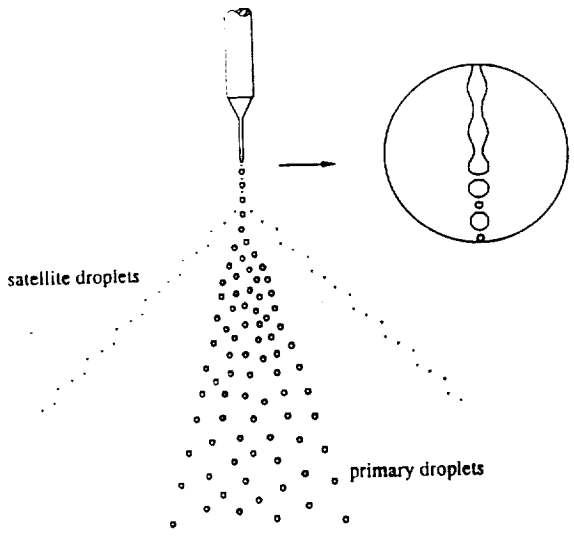

Fig. 1. Schematic of an electrospray.

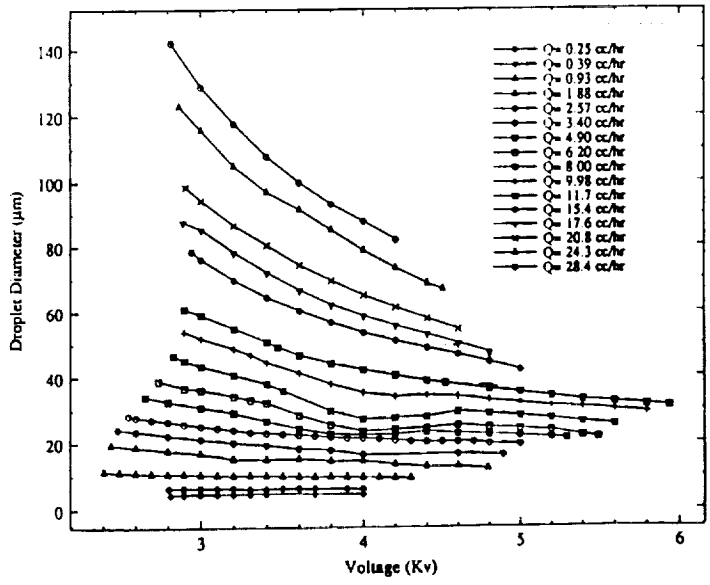

Fig.. 2 Droplet average diameter versus applied voltage for various liquid flow rates.

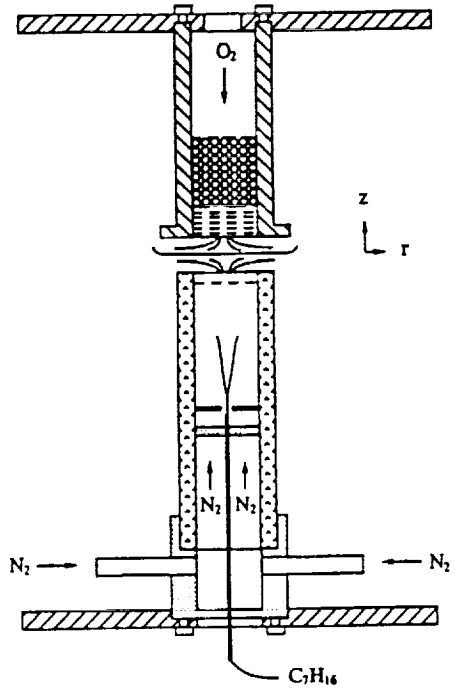

Fig. 3 Counteflow spray diffusion flame burner.

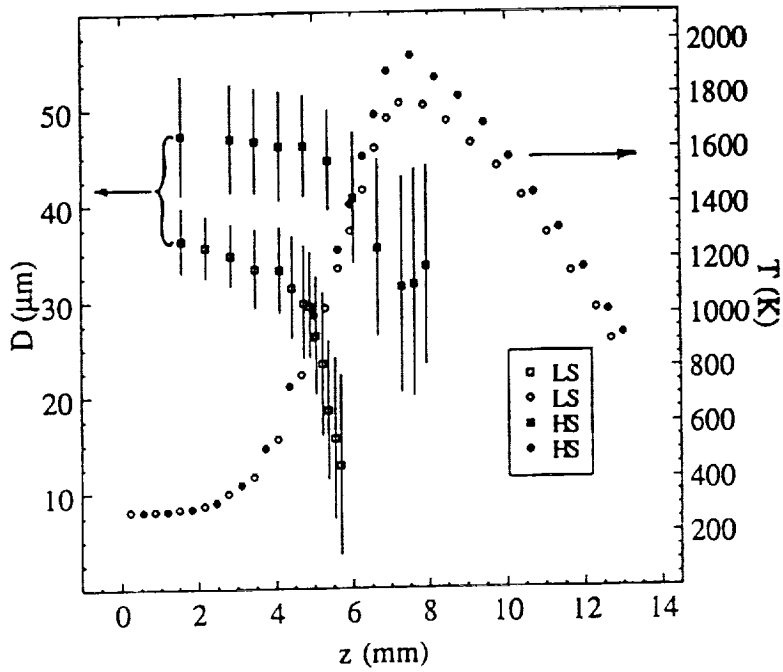

Fig. 4 Average droplet diameter (squares) and gas-phase temperature (circles) measured along the burner axis versus distance from the bottom burner rim.

Fig. 5 Microphotograph of a droplet in the act of disintegrating.

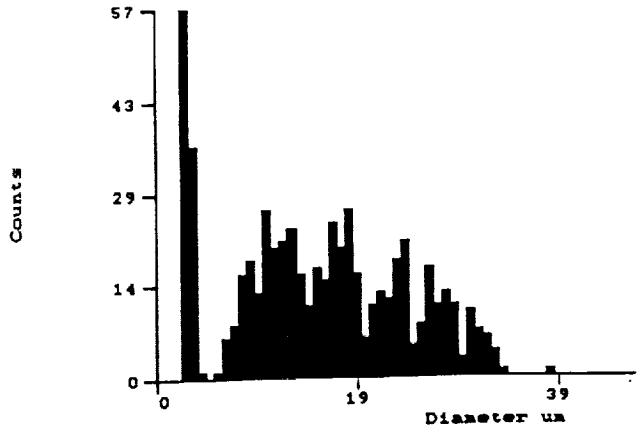

Fig. 6 Droplet size distribution measured at z=5.5 mm in Flame LS.

See Color Plate G-6